RSC Advances

ROYAL SOCIETY OF CHEMISTRY

www.rsc.org/advances

RSC Advances

RSCPublishing

ARTICLE

2,5-Dimethoxy 2,5-dihydrofuran crosslinked chitosan fibers enhances bone regeneration in rabbit femur defects

Cite this: DOI: 10.1039/x0xx00000x

Received 00th March 2014,
Accepted 00th January 2013

DOI: 10.1039/x0xx00000x

www.rsc.org/

Paulomi Ghosh, Arun Prabhu Rameshbabu, Nantu Dogra, Santanu Dhara*

Chitosan fibers were fabricated via pH induced neutralization and precipitation in 5 w/v% NaOH bath. Intermolecular covalent crosslinking of these fibers were performed through imine linkages between gluocosamine units of polymer and dialdehyde groups of 2,5-dimethoxy-2,5-dihydrofuran at 60°C, pH 2.2. The covalently crosslinked fibers demonstrated improved tensile strength, stiffness, hydrophobicity and higher stability against enzymatic degradation compared to uncrosslinked ones under wet condition. The differences in the physico-chemical characteristics were reflected in protein adsorption which in turn facilitated higher cellular proliferation and adhesion on the crosslinked fibers. Osteogeneis of human bone marrow derived mesenchymal stem cells (hMSCs) was significantly higher on crosslinked fibers compared to the uncrosslinked ones as evidenced by higher alkaline phosphatase expression, calcium deposition and osteocalcin secretion. *In vivo* study performed subcutaneously in a rabbit model with the crosslinked fibers revealed its ability to integrate with host tissues and showed differential extent of cellular infiltration and extracellular matrix production after specified periods of implantation. Further bone regeneration ability at the defect site filled with crosslinked fibers was evident by histological analysis. Thus, the study suggests that DHF crossliked chitosan fibers could be used for bone tissue engineering applications.

1. Introduction

Tissue engineering has emerged as a potential alternative to replace, repair, and regenerate malfunctioned or lost tissues/organs. In this approach, matrices/scaffolds of natural, synthetic and semi synthetic origin in combination with stem cells are being explored for a variety of restorative applications.[1] Besides providing mechanical support and tailorable biodegradability, a scaffold should also act as a template for cell adhesion, proliferation and differentiation.[2] Chitosan, an aminopolysaccharide, is reported for a wide range of therapeutic applications including scaffolds for regenerative medicine owing to its nontoxicity, biocompatibility and structural resemblance to glycosaminoglycans found in extracellular matrix.[3] Detailed account of differential cellular activities on various forms of chitosan such as fibers, films, hydrogels, beads and sponges are reported in literature.[4] Amongst all architecture types, fiber based scaffolds are favourable for bone tissue engineering as they provide high surface area, controlled porosity for cell migration and nutrient/waste transport.[5] Owing to higher surface area, fibrous scaffolds offer superior cell-material interactions in comparison to hydrogels.[6] Woo et al. reported that fibrous scaffolds adsorbed 4.2 fold greater amounts of serum proteins than solid walled scaffolds made from same material.[7] Moreover, the fibers can easily be filled at the injury site according to the defect profile and macroporosity related to interfiber space is favourable for cellular migration and tissue ingrowth.

The presence of amine and hydroxyl groups in chitosan facilitates rapid swelling and biodegradation in comparison to its native form (chitin). Thus, chitosan displays poor mechanical properties that are insufficient to match hard tissue engineering applications. Various crosslinkers are explored to provide improved mechanical strength and tunable biodegradation properties to chitosan.[8] Dialdehydes such as glutaraldehyde and glyoxal are the most common crosslinkers wherein the aldehydes crosslink glucosamine units of chitosan to form imine bonds via schiff base formation.[9] Nevertheless, glyoxal and glutaraldehyde are known to be mutagenic and neurotoxic in nature, respectively.[8] Acute peroral and/or percutaneous toxicity due to exposure to glutaraldehyde are well documented in literature.[10] Also, previous reports evidenced that reactions between chitosan and aldehydes, in particular glutaraldehyde occur rapidly, hence the reaction kinetics are difficult to control. For instance, gel formation of chitosan with glutaraldehyde was reported to take place within 1 min at 27 ˚C.[11] Alternative means of slowing and controlling crosslinking of chitosan is the use of a thermally-activated crosslinking agent, butenedial. The onset time and rate of the gelation of chitosan could be manipulated by controlling temperature, pH and butenedial concentration through the use of precursor molecule, 2,5-dimethoxy-2,5-dihydrofuran (DHF).

DHF is a non-toxic dialdehyde based crosslinker wherein the aldehyde groups form intermolecular imine linkages in a similar principle like other aldehyde crosslinking.[12] The extent of imine-mediated crosslinking offers tailorable swelling and biodegradability through modification of amine groups. Additionally, alkene moieties present in DHF could be amenable to further functionalization/bioconjugation with nucleotides and peptides in order to render them bioactive.
Though Johnson et al. investigated shape forming of ceramics and metal through gelation of chitosan with DHF, however chitosan was used as sacrificial material and was burnt out prior to sintering.[12b] DHF crosslinked amino-polysaccharides including chitosan have not yet been explored for bone regeneration using human bone marrow derived mesenchymal stem cells (hMSCs). Modulating scaffold characteristics could lead to differentiation of hMSCs along multiple cell lineages including osteogenic lineage with increased ALP expression, osteocalcin production and secretion of calcium crystals.[13]

In this study, DHF crosslinked chitosan fibers were fabricated and characterized for physico-chemical properties. Influences of physico-chemical properties of crosslinked fibers on osteogenic differentiation ability of hMSCs and *in vivo* compatibility upon subcutaneous implantation for two months through histological and histochemical studies were also assessed. Further, bone regeneration ability of crosslinked and uncrosslinked fibers were compared by implantation of the fibers at the orthotropic sites.

2. Experimental

2.1 Preparation of native and crosslinked chitosan fibers

Chitosan (MW 710000; > 90 % deacetylated, Marine chemicals, Cochin) 6 wt% stock solution was prepared in 2% v/v acetic acid (Merck, India). The homogenous polymer solution was filtered through a muslin cloth and deaired by centrifugation. Preliminary rheological studies were performed to assess gel formation with NaOH and DHF (see supplementary text). Based on the gelation kinetics, chitosan fibers were fabricated using a viscose type stainless steel spinneret (50 holes, 0.1 mm) in 5% w/v NaOH bath at pH 13; which were subsequently collected on a rotating collector. These chitosan fibers were then cross-linked covalently with different concentrations of DHF, pH 2.2 respectively to study the influence of crosslinking on physicochemical properties. Further, chitosan fibers formed in NaOH bath were also crosslinked with 5% glutaraldehyde at room temperature to compare mechanical stability and cell viability with the DHF crosslinked ones. The surface features of vacuum dried fibers before and after crosslinking were examined using scanning electron microscopy (SEM, Zeiss EVO 60, and Germany). Prior to observation on SEM, the fibers were mounted on metal grids and coated with gold under vacuum using plasma sputtering unit.

2.2 Characterization

2.2.1 FTIR

Chitosan fibers prepared at different conditions were examined using Fourier Transform Infrared (FTIR) spectrophotometer (Model NEXUS-870, Thermo Nicolet Coorporation, Madison, WI, USA) using KBr disk method over the wavelength range of 400-4000 cm^{-1} on a Perkin Elmer spectrophotometer.

2.2.2 Crosslinking density, swelling and biodegradation study

Crosslinking density, swelling and biodegradation study were performed as stated in the supplementary information.

2.2.3 Nanoindentation and tensile strength

Nanoindentation on crosslinked and uncrosslinked chitosan fibers was performed to obtain load-displacement and hardness data using Nanoindenter (TI 950 TriboIndenter, Hysitron Inc., USA) at maximum load of 100 µN with dwelling time period of 10 sec. A total number of 10 points at a distance of 4 µm was employed for the study. Mechanical testing of dry and wet fibers was performed under tensile mode in a universal testing machine (H25KS, Hounsfield, UK) with 25 N load cell at room temperature. Fibers (n=10) of gauze length 30 mm were pulled at 1mm/min. To determine wet strength, the fibers were allowed to swell overnight.

2.2.4 Water contact angle measurements

Characterization of fiber wettability was performed using sessile drop technique as reported in a previous study.[14] Protractor software was used to calculate the equilibrium angle formed between 2 µL of ultra high pure water drop and surface of the fibers (n=3).

2.3 Protein adsorption

Protein adsorption on chitosan fibers was performed as reported by Datta et al.[15]

2.4 Cell culture studies

hMSCs were purchased from Advanced Neuro-Science Allies (ANSA) Bangalore, India, where routine characterization of hMSCs for surface markers expression is studied. The hMSCs were positive for CD 90, CD 73, and CD 44. hMSCs were expanded in complete medium consisting of α-MEM supplemented with 10% FBS, 1% penicillin/streptomycin solution and 3.7% sodium bicarbonate (all Himedia) at 37 °C in a 5% CO_2 atmosphere. Subculturing was done on every 4th day by detaching cells with trypsin-EDTA and cell count was performed using countess (Invitrogen). For cell seeding studies, equivalent weight of chitosan fibers were placed in 24 well plates. The fibers were sterilized and washed with PBS repeatedly. After aspiration of PBS, fibers were incubated with complete medium. The media was then removed and hMSCs were seeded at a density of 10^4 cells cm^{-2} of chitosan fibers. After 24h, fibers with cells were transferred to a new well plate to minimize error during proliferation and differentiation assays. Cells were also seeded in tissue culture plates and used as positive control. After 2 days, cells seeded on chitosan fibers were cultured in osteogenic induction medium containing 100 nM dexamethasone, 0.2 mM ascorbic acid and 10 mM glycerophosphate for different time periods. Media changes were performed after 24 h and every 48 h thereafter.

2.4.1 Cell proliferation, viability and morphology

DNA quantification assay was performed with Hoechst 33258 (Sigma, St. Louis, MO) to assess hMSC proliferation. The cells adhered on the fibers were trypsinised for 30 mins followed by incubating the cells in lysis buffer (0.5% Triton X-100, 20 mM Tris-HCl, 1 mM EDTA, 100 mM NaCl, pH 8.0). Hoechst solution (0.1 mg/ml) was added to the cell lysate and placed in cuvette. Florescence intensity was measured using fluorescence spectrophotometer. A DNA standard curve was obtained from a known number of cells.
Viable MSCs adhered on the crosslinked and uncrosslinked fibers were assessed by MTT (3-(4, 5-Dimethylthiazol-2-yl)-2, 5-diphenyltetrazolium bromide, Sigma Aldrich) assay after 1, 3 and 7 days of seeding according to a previous report.[7]

Morphology of adherent cells on the fibers was examined using SEM, florescent and bright field imaging. For florescent

imaging, cells at 3rd day were fixed with 3.7% paraformaldehyde, followed by repeated washing with PBS, 7.4. Cell nuclei were stained with DAPI (molecular probes) and imaged in Axiovision research microscope (Carl Zeiss, Germany).

2.4.2 Cell differentiation assays

Cell differentiation was assessed using ALP, osteocalcin ELISA and alizarin assay.

ALP assay

For alkaline phosphatase activity, cells on crosslinked and uncrosslinked fibers were lysed in PBS containing 0.1 M glycine, 1 mM $MgCl_2$ and 0.05% Triton X-100 at specific time intervals (7, 14 and 21 days). This was followed by incubation with p-nitrophenyl phosphate solution (pNPP) at 37 °C for 30 min. ALP activity was stopped by adding NaOH. The amount of p-nitrophenol (pNP) that corresponds to alkaline phosphatase activity was measured at 405 nm. The ALP activity of hMSCs was expressed as nmol of pNP/reaction time/total protein (nmol/min/total protein).

Osteocalcin ELISA

Osteocalcin production from hMSCs cultured on crosslinked/uncrosslinked fibers after 14 and 21 days was determined by commercial enzyme immunoassay kit (Invitrogen, USA) as per manufacturer`s instructions.

Alizarin red assay

Calcium deposition on chitosan fibers were assessed quantitatively as well as by histochemical staining.

2.5 *In vivo* studies

2.5.1 Implantation of fibers in rabbit model

In vivo biocompatibility of chitosan fibers were performed under the compliance of Institutional Animal Ethical Committee guidelines of Indian Institute of Technology Kharagpur, India. Briefly, New Zealand white male rabbits weighing approximately 1 kg (n = 5) were maintained in a well aerated atmosphere with adequate diet supplements. Rabbits were anesthetized with injections of ketamine hydrochloride prior to start of experiment. For subcutaneous biocompatibility study, 4 cm incision was made in the dorsal skin of the rabbits to insert chitosan fibers. The incision was closed using sutures and care was taken to prevent post-operative infections. Rabbits were sacrificed after specified time period and the surrounding tissue near the subcutaneous implants was retrieved and fixed in 10% neutral buffered formalin solution (Merck, India).

To assess bone formation *in vivo*, defects (2.5 mm in diameter) were drilled on one side of femur. Fibers of appropriate size were inserted into the defect site using press fit. The defect site was closed using suture. After 6 weeks, rabbits were sacrificed and fibers implanted in bone were retrieved with surrounding tissues and fixed in formalin. Tissues with fibers were further decalcified with 10% ethylene diamine tetraacetic acid.

2.5.2 Histology and histochemistry

The samples were dehydrated in ethanol series, passed through xylene and embedded in paraffin. Sections of 3 µm thickness were sliced for both subcutaneous and bone implantation followed by hematoxylin-eosin staining. Collagen I (Abcam) staining was performed following manufacturer`s instructions. Von Kossa staining was also performed for detecting calcium deposition in bone sections.

2.6 Statistical analysis

All experiments were done in triplicates. Data were expressed in mean ± standard deviation. Statistical analysis was carried out using t-test and p value of 0.05 was considered significant.

3. Results and discussion

3.1 Preparation of chitosan fibers

Chitosan dissolved in acidic media readily formed hydrogel when exposed to alkaline condition as evidenced by increase in complex viscosity (supplementary Fig. S1a). Mechanistically, glucosamine units of chitosan are protonated when dissolved in acetic acid, which promotes gelation/precipitation of the polymer via pH induced neutralization in alkaline solution. This instantaneous gel forming ability of chitosan in alkaline condition was successfully used for fiber formation via wet spinning using viscose type spinneret. Fig. 1a shows SEM of uncrosslinked chitosan fiber formed in NaOH bath. However, gelation kinetics of chitosan with DHF is slow and is temperature mediated (supplementary Fig S1b). Consequently, *in situ* crosslinking and fiber formation could not be achieved in DHF bath. Therefore, chitosan fibers formed in NaOH bath were crosslinked in an additional step with different concentrations (3, 5, 10% v/v) of DHF to obtain crosslinked chitosan fibers with tailorable crosslinking densities. Representative SEM micrograph of chitosan fiber crosslinked with 5% v/v DHF at 60 °C is shown in Fig. 1b. The crosslinked fibers were smooth in appearance and retained their integrity after crosslinking. On the other hand, formation of fibers at higher concentration and temperature led to crumbling of the fibers. Fig. 1c shows brittleness of chitosan fibers formed with 10% v/v DHF at 80°C. Fig. 1d shows flexibility of fibers crosslinked with 5% v/v at 60°C. Chitosan fibers formed in NaOH bath were also crosslinked with 5% v/v glutaraldehyde to compare with DHF crosslinked fibers. The glutaraldehyde crosslinked fibers lacked mechanical stability and were brittle in nature (data not shown).

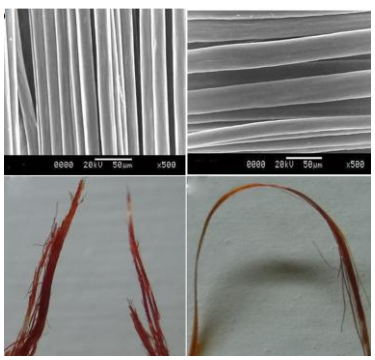

Fig.1 Chitosan fiber formation in NaOH solution and their crosslinking with DHF. Representative SEM micrographs showing (a) uncrosslinked and (b) DHFcrosslinked chitosan fibers. Optical images of chitosan fiber crosslinked with DHF (c) 10% v/v, 80℃ and (d) 5% v/v, 60℃ demonstrating brittleness and flexibility, respectively.

3.2 Characterization

3.2.1 FTIR

Chitosan fibers were characterized by FTIR spectroscopy as shown in Fig. 2a. The peaks for glucosamine unit of chitosan at 900 cm^{-1}, 1030 cm^{-1}, 1080 cm^{-1} and 1153 cm^{-1} are present in both uncrosslinked and crosslinked fibers. The peaks around 1378 cm^{-1} ,2996 cm^{-1} and 3440 cm^{-1} corresponds to the O- stretching, C-H stretching and O-H stretching, respectively. Further, the peak values around 1420 cm^{-1} and 1390 cm^{-1} are attributed to -CH_2- wagging. The FTIR spectra of uncrosslinked fiber shows characteristic band of amide I (1657 cm^{-1}) due to C=O stretching and amide II (1590 cm^{-1})

due to N-H in plane deformation. Crosslinking of chitosan fibers with DHF resulted in appearance of three new bands : 1650 cm^{-1} indicated presence of imine (C=N) stretching band, 1566 cm^{-1} and 3100 cm^{-1} could be attributed to the presence of ethylenic (C=C) and =C-H stretching, respectively. The appearance of these new peaks is due to crosslinking of dialdehydes of DHF with glucosamine units of chitosan forming Schiff base.[16] Additionally crosslinking was evidenced by absence of peaks of aldehyde at 1720 cm^{-1} and reduction of intensity of amine moieties at 1590 cm^{-1} in the crosslinked fibers. This is in agreement with previous reports.[17] Further, presence of three conjugated double bonds could be ascertained by the appearance of orange-reddish color on the fibers (Table 1). The higher the concentration of DHF, the more was the degree of crosslinking and formation of imine linkage induced conjugations and accordingly a deeper shade was attained for the crosslinked fibers. The scheme for fiber formation in alkaline bath and their crosslinking with DHF is depicted in Fig. 2b.

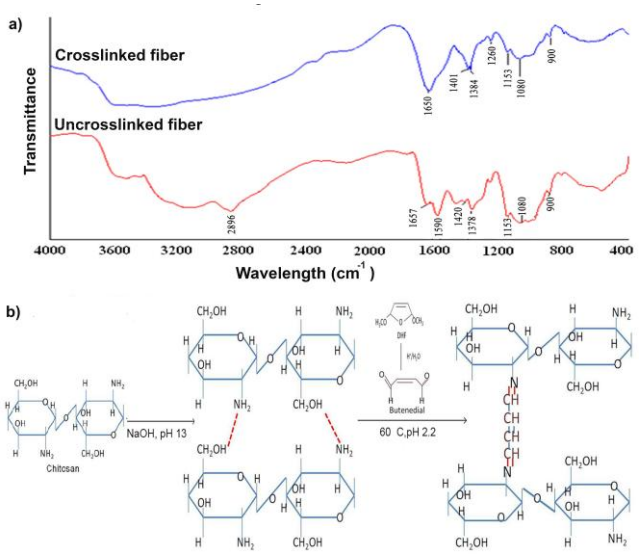

Fig.2 a) FTIR spectra of crosslinked and uncrosslinked chitosan fibers. b) Schematic representation of chitosan based fiber formation in (a) NaOH bath at pH13 by hydrogen bonding, b) covalent crosslinking reactions with DHF at 60 ˚C, pH 2.2

3.2.2 Crosslinking density, swelling and biodegradation properties

Ninhydrin assay was used to determine the degree of crosslinking of the fibers as shown in Table 1. The crosslinking density increased from 35 to 84% upon increasing the concentration of DHF from 3 to 10% v/v. Thus, it was evident that higher the crosslinker concentration, more was the crosslinking density of the fibers. The crosslinking density of 5% v/v glutaraldehyde crosslinked chitosan fibers was found to be 86% which was more than 10% DHF crosslinked fibers. This may be because crosslinking of chitosan with glutaraldehyde is rapid; in contrast, crosslinking of DHF is mediated by the formation of an intermediate, butenedial making the reaction slower. Thus, higher crosslinking densities were achieved with glutaraldehyde than with DHF after same time interval. This subsequently affected mechanical stability of the fibers. The 5% v/v glutaraldehyde crosslinked fibers were brittle in nature.

The degree of swelling and rate of biodegradation are presented in Table 1. Uncrosslinked fibers swelled the most (168%) after 24h while crosslinked fibers demonstrated restricted % swelling. One of the primary factors that govern % swelling is the degree of crosslinking. This was evidenced in our study by the reduction in % swelling from 105 to 80% as degree of crosslinking increased from 35% to 84%. Swelling is an essential decisive factor while fabricating scaffolds for tissue engineering as it dictates mechanical integrity under wet condition.[18] Also, crosslinking has direct influence on rate of biodegradation. After 4 weeks of lysozyme treatment, the percent weight remaining of crosslinked fibers was significantly higher than uncrosslinked ones (45%) as shown in Table 1. This may be because crosslinking via imine linkages improved mechanical stability. However, there was no significant difference in rate of degradation of the fibers crosslinked with 5 and 10 vol% of DHF.

Table 1: Physical appearance, degree of crosslinking, swelling and biodegradation characteristics of chitosan fibers crosslinked with different concentrations of DHF at 60 °C and their comparison with uncrosslinked ones

DHF v/v%	colour	% CD	% Swelling*	% weight remaining**
0	White	N/A	168±4.1	45
3	orange	35	105 ± 6	62
5	Red	62	88 ± 5.2	72
10	Deep red	84	80.7 ± 7	77

CD = crosslinking density; N/A = not applicable; * after 24h; ** After 35 days

For further study, chitosan fibers crosslinked with 5% v/v DHF was chosen due to its better shape retention, fiber morphology and less brittleness yet high strength, favorable degree of swelling and degradation kinetics. The crosslinked fibers were compared with uncrosslinked ones to demonstrate influence of crosslinking on mechanical and biological properties. The uncrosslinked and crosslinked fibers were named ChN and ChD, respectively.

3.2.3 Nanoindentation measurements and tensile strength

Mechanical properties of chitosan fibers are depicted in Fig. 3. ChD demonstrated less change in displacement than ChN indicating more stiffness when equivalent load was applied (Fig. 3a). ChD displayed reversible displacement of 700 nm under 100 µN load with permanent deformation of ~150 nm. On the contrary, ChN had very low elastic limit with 1000 nm reversible displacement and 400 nm permanent deformation under the same load. The average hardness values for ChD and ChN were 38.4 ± 1.73 MPa and 11.5 ± 2.8 MPa, respectively (Fig. 3b). This is in agreement with previous reports where crosslinking of chitosan films endowed significant high hardness values.[19] Tensile strength of chitosan fibers at dry and wet conditions are shown in Fig. 3c. Tensile strength of dry ChD (60 ± 1.09 MPa) was less than dry ChN (100 ±2.06 MPa). This may be because covalent crosslinking of chitosan fibers with DHF under swelling condition resulted in less degree of crystallinity as the crosslinking reaction interrupted intermolecular H-bonding and subsequently hindered compaction during drying. However, it is important to note that tensile strength of ChD under wet condition (43 ± 2.51 MPa) was comparatively higher than ChN (30 ± 2.13 MPa) associated with less swelling of crosslinked fibers. As the crosslinked fibers have higher wet strength than uncrosslinked fibers, they could be more suitable for intended applications under wet condition.

3.2.6 Contact angle measurements

Wettability of ChD and ChN is shown in Fig. 3d. Contact angles for ChD and ChN were 80°and 55°, respectively. As higher number of the amine (NH_2) functionalities were utilized for covalent crosslinking in ChD fibers, they could not undergo hydration with

water to a same extent as in uncrosslinked ones. This endowed remarkable hydrophobicity in ChD. This is in agreement with previous reports regarding aldehyde crosslinked chitosan.[9a]

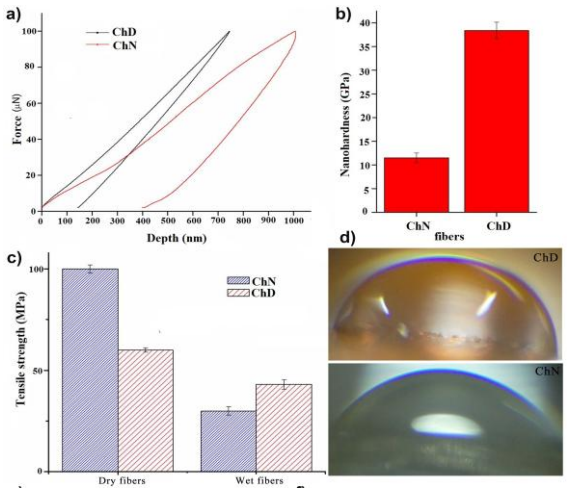

Fig.3 Studies of mechanical properties and wettability of crosslinked, ChD and uncrosslinked, ChN chitosan fibers. a) Load-displacement, b) Hardness, c) Tensile strength in dry and wet conditions and d) Water contact angle measurements.

3.3 Protein adsorption

Protein adsorption on ChD and ChN after 1 and 16 hours respectively is shown in Fig. 4a. The graph clearly indicates that adsorption of serum protein from media was marginally lower for ChD after 1h but increased significantly after 16h incubation. Notably, water molecules from aqueous biological environment interact with materials even before proteins could adsorb onto a material surface.[20a] In case of hydrophobic materials, a shell of water molecules forms that interacts with each other more than with hydrophobic surfaces forming a stable state with reduction in entropy. Disruption of this layer with proteins is energetically favorable as it increases the entropy of the system. As a result, proteins have high affinity towards hydrophobic surface and are adsorbed more in comparison to charged hydrophilic surfaces. Further, proteins tend to unfold and spread its hydrophobic core over the biomaterial surface to minimize the net hydrophobic surface area of the system exposed to the solvent in order to achieve thermodynamic equilibrium.[20] Accordingly in our study, crosslinked fibers with more surface hydrophobicity than uncrosslinked ones depicted higher protein adsorption after 16h. The protein adsorbed in turn interacts with cell surface molecules like integrins, thereby, modulating adhesion of anchorage dependent cells.

3.4 Cell culture studies

3.4.1 Cell proliferation, viability and morphology

To assess cell proliferation, change in DNA content was measured after specified time intervals (1st, 3rd and 7th day). DNA amount increased with increase in incubation period for both the scaffolds; cells on ChD displayed higher proliferation efficiency (Fig. 4b). Cell viability was measured by MTT reduction assay as shown in Fig. 4c. Both ChD and ChN maintained viable population of hMSCs throughout the study period and showed increase in rate of proliferation with increase in time. Cell density was similar after 4 h of seeding for both the fibers; though after 24h, ChD displayed marginally higher cell number compared to ChN. After 3 days of culture, ChD showed higher rate of proliferation than ChN. After 7 days, ChD and ChN fibers supported 6.8 x 10^5 cells ± 0.0293 and 3.72 x 10^5 ± 0.019 cells, respectively. Wettability of biomaterials plays an important role in cell adhesion. Polymer surfaces with a water contact angle of 70˚ were reported to provide the most appropriate surface for cell attachment. Highly hydrophilic surfaces bind weakly to the adsorbed proteins, which could lead to detachment of these proteins in long term cell culture.[21] Hence, moderately hydrophilic surfaces are desirable for optimal cell adhesion. However, cell adhesion to a material`s surface is a complex event and is influenced by other factors such as surface charge, chemical cues, topography, cell type, besides wettability of the biomaterial.

Cell viability of glutaraldehyde crosslinked fiber was also evaluated to compare cellular growth kintetics with ChD. Similar rate of proliferation was achieved at initial period on both the covalently crosslinked fibers (Fig. S2). However, at later period, cell viability was higher for ChD than for glutaraldehyde crosslinked fibers. After 7 days, cell density was 2.4 x 10^5 as against 6.8 x 10^5 cells for ChD. This may be due to toxicity associated with higher rate of cell death in glutaraldehyde crosslinked fibers. This is in agreement with previous reports.[8,9] Glutaraldehyde crosslinked fibers were excluded from further studies due to slow growth kinetics of cells on them.

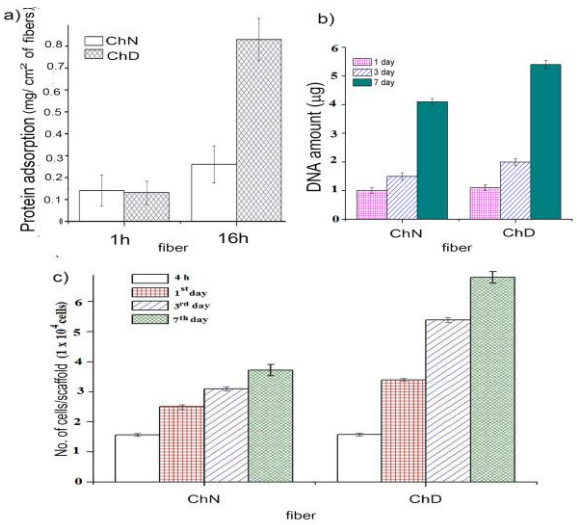

Fig.4 In vitro studies a) Comparative study of protein adsorption after 1and 16 hours; b) DNA quantification of hMSCs at 1st, 3rd and 7th day; c) Cell viability after 1, 3 and 7 days. Values represent Mean ± SD (n=3). $P < 0.05$

The higher cellular density on DHF crosslinked fibers was further supported by SEM images (Fig. 5a, b). SEM images revealed higher coverage of cells on ChD fibers in comparison to the uncrosslinked ones and both the samples showed stretched morphology of hMSCs after 7 days. Similar to SEM, florescent images showed higher number of cells attached to ChD than ChN after 3 days of seeding (Fig. 5c, d). The inset shows respective bright field images of cells on fibers. Thus, DHF crosslinked fibers have better cellular attachment, viability and proliferation rates compared to uncrosslinked fibers.

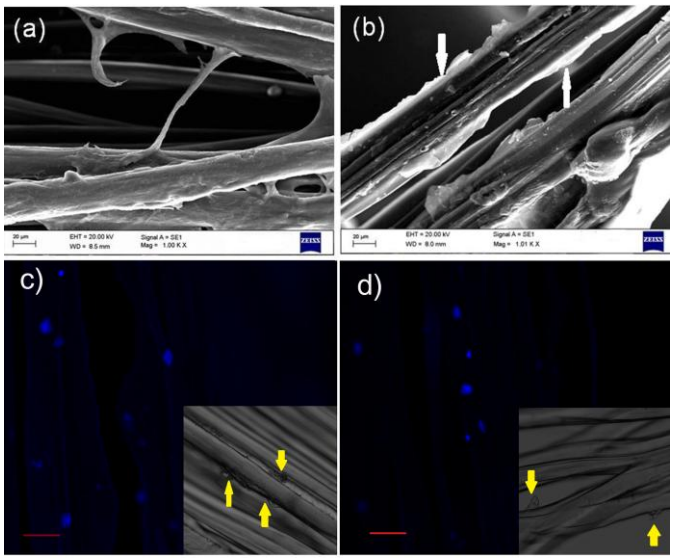

Fig.5 hMSC adhesion on chitosan fibers. SEM images of hMSCs adhered on a) uncrosslinked, ChN; b) Covalently crosslinked, ChD fibers at 7th day. The white arrows represent sheet of hMSCs adhered on ChD fibers. The scale represents 20 µm. Florescent images of hMSCs adhered on fibers c) ChD and d) ChN, respectively. Inset represents bright field images of cells on the respective fibers. The scale represents 40 µm.

3.4.2 Cell differentiation assay

Alkaline phosphatase is a membrane bound enzyme which hydrolyses phosphate ester thereby increasing local phosphate concentration; the inorganic phosphate contributes to the differentiation of stem cells.[22] Hence ALPase, is widely recognized as an early phenotypic marker for osteoblast differentiation. The early osteoblastic differentiation of hMSCs on ChD and ChN was determined using ALP enzymatic activity at different time periods as shown in Fig. 6a. ALPase activity was normalized against total protein which is a measure of rate of cell proliferation. In our study, the ALPase activity increased with time for both the chitosan based fibers indicating switching of mesenchymal stem cells from growth to differentiation phase. Pnp expression was highest for covalently crosslinked fibers at all time periods ($p< 0.005$). ALPase activity was 53.04 ± 0.28 and 32.23 ± 0.43 nmol/min/mg of total protein after 21 days of culture for ChD and ChN, respectively.

The high ALP activity on crosslinked fibers coincided with greater levels of osteocalcin (OC) expression at 21 days as derived from ELISA assay. After 3 weeks, OC on ChD were 75.6 ± 0.9 ng/ ml when compared to 24 ± 0.5 ng/ ml in uncrosslinked ones (Fig. 6b). Osteocalcin is a calcium binding protein that is highly expressed in differentiated cells during mineralization stage. In the present study, OC expression was prominent only after 14 days.

Alizarin red assay was used to evaluate mineralization on the chitosan fibers after 21 days of culture as shown in inset of Fig. 6b. A complex forms between calcium and alizarin red dye due to chelation, the end product of which is birefringent.[23] The optical density of the dye upon extraction after 21 days of culture for ChD was observed to be 1.2 while it was only 0.19 for ChN. Nodule formation was qualitatively higher both in terms of distribution and size on ChD than on ChN indicating greater extent of mineralization on crosslinked fibers. Mineralization refers to secretion of extracellular calcium and phosphorus salts by the cells at nucleation sites known as matrix vesicles present in the lacunae of cartilage leading to calcification. The accumulated Ca^{2+} and inorganic phosphate serve as nucleating agents for the formation of hydroxyapatite, the main inorganic component of bone.[24] A recent study by Pati et al. showed that fibrous chitosan scaffolds crosslinked with tripolyphosphate supported enhanced mineralization than that of uncrosslinked fibers after 3 weeks of culturing.[25] However, due to phosphate ions already present on the fibers, mineralization of chitosan-TPP fiber surfaces may be due to both cellular differentiation and polymer based calcification. On the other hand, presence of calcium on ChD fibers lacking phosphate and calcium ions in its structure indicated that hMSCs adhered on the fibers underwent maturation and encouraged mineral deposition. Overall, it was observed that hMSCs on crosslinked chitosan fibers exhibited higher levels of differentiation in terms of ALP activity, greater expression of osteocalcin as well as calcium secretion.

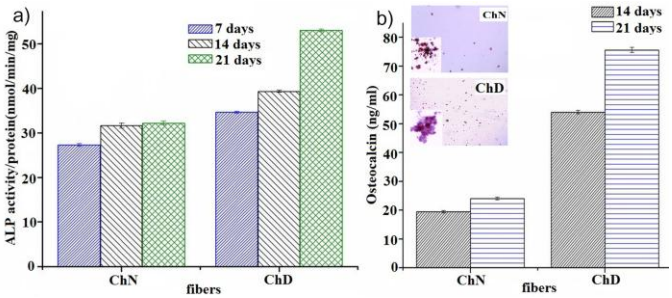

Fig.6 Cell differentiation assays a) ALP activity of hMSCs after 7, 14and 21 days (n=3, $P < 0.05$) and d) Osteocalcin ELISA assay after 14 and 21 days (n=3, $P < 0.05$) adhered on ChN and ChD fibers. Inset depicts optical images of alizarin red assay at 21st day on ChN and ChD fibers showing distribution of calcium deposition and nodule size.

3.5 *In vivo* studies

3.5.1 Subcutaneous biocompatibility studies

In vivo biocompatibility of crosslinked and uncrosslinked chitosan fibers were evaluated via subcutaneous implantation in rabbits. Fig. 7a shows representative image of bundle of fibers implanted in the subcutaneous layer. Optical images of retrieved fibers with muscular attachments are shown in Fig. 5b,c. Further, the retrieved fibers showed insignificant inflammation/infection in the operative site.

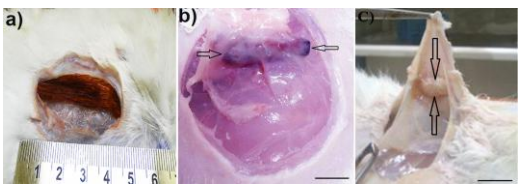

Fig.7 In vivo compatibility studies of chitosan fibers upon subcutaneous implantation in rabbits. Representative optical images of a) fibers before implantation; b) crosslinked and c) uncrosslinked fibers after retrieval. Scale bar represents 1 cm.

In vivo degradation and foreign body response of the retrieved chitosan fibers and surrounding tissues were evaluated by H & E staining (Fig. 8). After 6 weeks, ChN had almost degraded while sufficient amount of imine crosslinked fibers (ChD) were still visible. This is consistent with *in vitro* degradability of the fibers (Table 1). Presence of multinucleated giant cells indicates cell mediated degradation in addition to lysozyme mediated biodegradation of the chitosan fibers. Further, inflammatory reactions towards the polymer were characterized by the development of fibrous layer surrounding the implants after 2 weeks of implantation. However, the thickness of the fibrous layer decreased after 6 weeks for both the fibers. Infiltration of the host cells surrounding the

crosslinked fibers was evident. Additionally, higher number of blood vessels was seen surrounding ChD fibers (Fig. 8).

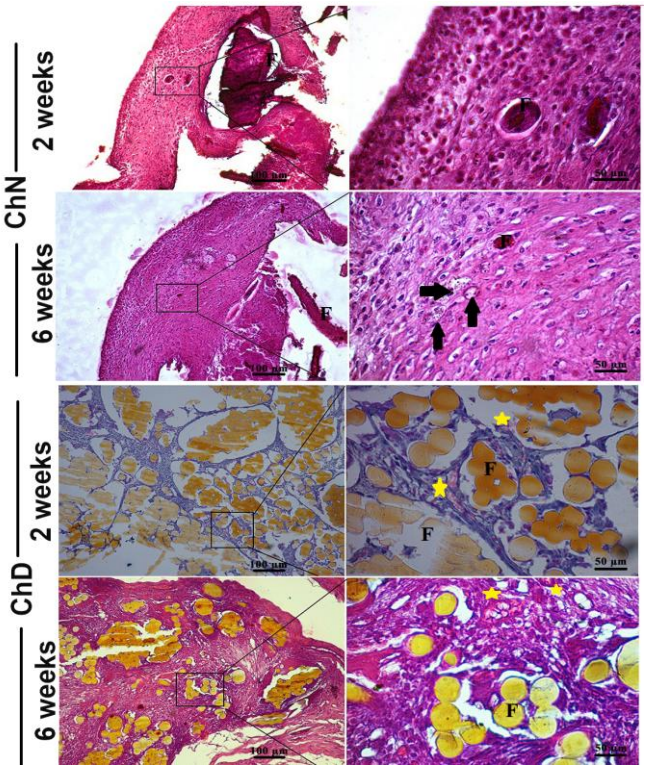

Fig.8Representative hematoxylin–eosin stained sections depicting *in vivo* host response to crosslinked, ChD and uncrosslinked, ChN chitosan fibers implanted subcutaneously in rabbit model. (F,fibers; arrow, macrophages or giant cells with multiple nuclei and star, blood vessels). Scale bar for lower magnification image on left panel is 100 µm and higher magnification image on right panel is 50 µm.

Immunohistochemistry for collagen I secreted by the surrounding cells is shown in Fig. 9. Immunohistochemistry results demonstrated immunopositivity for type I collagen to varying extents for ChD and ChN, respectively. Evidently, the area stained and intensity of type I collagen was visibly more for crosslinked fibers when compared to ChN. The presence of collagen I as a tissue response to implanted scaffold is used as a biocompatibility criteria.[28]

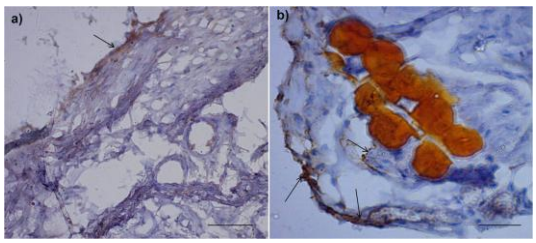

Fig.9 Immunohistochemistry of collagen I secreted by cells surrounded by a) uncrosslinked (ChN) and b) crosslinked (ChD) fibers. (arrows, collagen I). Scale bar represents 50 µm.

3.5.2 Bone growth supported by crosslinked chitosan fibers

To investigate the contribution of chitosan fibers on bone tissue regeneration, 2.5 mm defects in rabbit femur bones were drilled (Fig. 10a, b) and crosslinked/uncrosslinked fibers were inserted. At 1 week post-drilling, regeneration was similar for the fiber-filled and the empty control groups (data not shown). However, after 6 weeks, the defects treated with both the chitosan fibers showed higher levels of regeneration compared to the empty control (Fig. 10c,d). This is due to osteoconductive nature of chitosan. Previous reports suggested that chitosan can act as a template to guide new bone formation. However, rapid degradation of the polymer necessitates crosslinking with non toxic agents. Glutaraldehyde being toxic to the cells was thus eliminated from *in vivo* studies. At 4 weeks, limited calcified areas in ChN filled defect was observed; whereas woven bone (Fig. 10d1) with numerous osteocytes of various size and shape was evident surrounding ChD fibers. In addition, intense osteoblastic activity was evident on the woven bone surrounding ChD fibers. Mineralisation of the fibers was assessed by von Kossa staining of sections. The uncrosslinked fibers didn't show any calcium deposition (data not shown) in contrast the DHF crosslinked fibers facilitated calcium deposition as evidenced by Fig. 10d2.

Thus, the process of regeneration in the wound that was filled with crosslinked fiber was significantly faster than that for uncrosslinked ones.

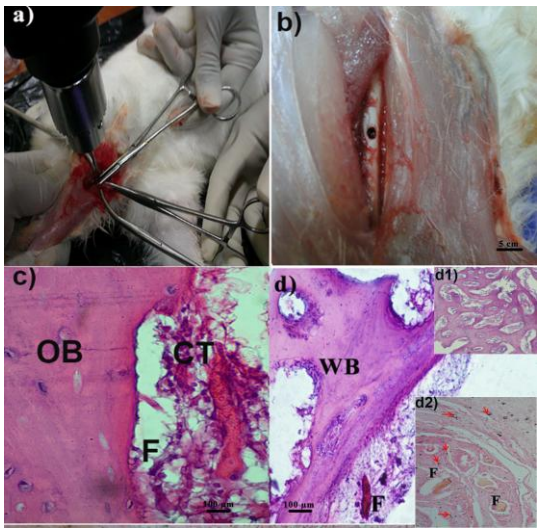

Fig.10 *In vivo* bone regeneration studies. a) Drilling of bone; b) Formation of 2.5 mm bone defect; H & E section of defect site implanted with c) uncrosslinked fibers and d) crosslinked fibers. Inset d1 shows formation of woven bone in the defects filled with uncrosslinked fibers; inset d2 shows mineralization of the newly formed bone as detected by von kossa assay (CT, connective tissue; F, fiber; OB, old bone; WB, woven bone; red arrow, mineralization).

In the present study, crosslinking of the native fibers influenced swelling, rate of degradation, wettability and mechanical properties that in turn influenced cellular differentiation. The enhanced maturation of hMSCs on crosslinked chitosan fibers and *in vivo* studies indicate their suitability for tissue engineering applications.

4.Conclusions

In this study, optimization of gelation kinetics of glucosamine units of chitosan with dialdehydes of DHF was successfully carried out. However, *in situ* fiber formation and crosslinking with DHF were not feasible in one step due to slow reaction kinetics of imine reactions. Therefore, chitosan fibers formed by precipitation in alkaline bath were crosslinked with DHF. The imine linkages formed after covalent crosslinking were confirmed by FTIR. The degree of crosslinking, brittleness, swelling

and rate of degradation was controlled by manipulating crosslinker concentration and temperature. The optimized crosslinked fibers had hardness of 38.4 ±1.73 MPa, wet strength of 43 ± 2.51 MPa and demonstrated moderately hydrophobic character. Covalently crosslinked fibers demonstrated enhanced proliferation of hMSCs and differentiation towards osteogenic lineage compared to uncrosslinked fibers. This was evidenced by ALP expression, calcium depositions and osteocalcin secretions. The covalently crosslinked DHF fibers were also compared with covalently crosslinked glutaraldehyde fibers. Glutaraldehyde crosslinked fibers lacked mechanical stability and were brittle; moreover their toxicity *in vitro* conditions were evident on 7th day of culture. In contrast, cell cultured on DHF crosslinked fibers were viable upto 21 days and could well differentiate into osteogenic linkage. The DHF crosslinked fibers supported better cellular infiltration and higher collagen I secretion than uncrosslinked fibers *in vivo* when subcutaneously implanted. In addition, DHF crosslinked fibers supported faster bone regeneration than uncrosslinked fibers, indicating their potential for bone tissue engineering applications.

Acknowledgements

Fellowship from Council of Scientific and Industrial Research (CSIR), Govt. of India, New Delhi is acknowledged for Paulomi Ghosh and Arun Prabhu Rameshbabu. Financial aid from Defence Research & Development Organisation (DRDO), and CSIR, Govt. of India, New Delhi is acknowledged.

Notes and References

Biomaterials and Tissue Engineering Laboratory
School of Medical Science and Technology
Indian Institute of Technology Kharagpur
Kharagpur- 721302, India.
*Corresponding author : sdhara@smst.iitkgp.ernet.in

1. (a) S. Bhumiratana and G. Vunjak-Novakovic, Stem Cells Transl. Med., 2012, 1, 64–69; (b) A. J. Oppenheimer, J. Mesa and S. R. Buchman, J. Craniofac. Surg., 2012, 23, 30–36.

2. A. R. Costa-Pinto, R. L. Reis and N. M. Neves, Tissue. Eng. Part B Rev., 2011, 17, 331–347.

3. (a) A. D. Martino, M. Sittinger and M. V. Risbud, Biomaterials, 2005, 26, 5983–5990; (b) R. A. A. Muzzarelli, Carbohyd. Polym., 2009, 76, 167–182; (c) M. N. V. R. Kumar, React. Funct. Polym., 2000, 46, 1–27.

4. I. Y. Kim, S. J. Seo, H. S. Moon, M. K. Yoo, I. Y. Park, B. C. Kim and C. S. Cho, Biotechnol. Adv., 2008, 6, 1–21.

5. (a) S. Z. Yow, C. H. Quek, E. K. Yim, C. T. Lim and K. W. Leong, Biomaterials, 2009, 30, 1133–1142; (b) A. C. Wan, E. K. Yim, I. C. Liao, C. L Visage and K. W. Leong, J. Biomed. Mater. Res. A., 2004, 71, 586–595.

6. N. Romano, D. Sengupta, C. Chung and S. C. Heilshorn, Biochim. Biophys. Acta., 2011, 1810, 339–349.

7. K. M. Woo, V. J. Chen and P. X. Ma., J. Biomed. Mater. Res. A., 2003, 67, 531–537.

8. J. Berger, M. Reist, J. M. Mayer, O. Felt, N. A. Peppas and R. Gurny, Eur. J. Pharm. Biopharm., 2004, 57, 19–34.

9. (a) M. M. Beppu, R. S. Vieira, C. G. Aimoli and C. C. Santana, J. Membr. Sci., 2007, 301, 126–130; (b) M. N. Khalid, J. L. Agnely, N. Yagoubi, J. L. Grossiord and G. Couarraze, Eur J Pharm Sci., 2002, 15, 425–432.

10. B. Ballantyne and S. L. Jordan, J. Appl. Toxicol., 2001, 21, 131–151.

11. T. Y. Hsien and G. L. Rorrer, Ind. Eng. Chem. Res., 1997, 36, 3631–3638.

12. (a) E. W. Hansen and K. H. Holm, Polymer, 1997, 38, 4863–4871; (b) S. Johnson, D. E. Dunstan and G. V. Franks, Colloid Polym. Sci., 2004, 282, 602–612. (c)S. Johnson, D. E. Dunstan and G. V. Franks, J. Am. Ceram. Society, 2002, 85, 1699–1705.

13. (a) A. I. Caplan, J. Orthop. Res. 1991, 19, 641–650; (b) M. F. Pittenger, A. M. Mackay, S. C. Beck, R. K. Jaiswal, R. Douglas, J. D. Mosca, M. A. Moorman, D. W. Simonetti, S. Craig and D. R. Marshak, Science, 1999, 284, 143–147; (c) C. Vater, P. Kasten and M. Stiehler, Acta Biomater., 2011, 7, 463–477.

14. (a) N. Sachot, O. Castaño, M.A. Mateos-Timoneda, E. Engel and J.A. Planell, J. R. Soc. Interface., 2013, 10, 20130684; (b) N. Bhardwaj and S. C. Kundu, Carbohyd. Polym., 2011, 85, 325–333.

15. P. Datta, J. Chatterjee and S. Dhara, Colloids Surf. B Biointerfaces., 2012, 94, 177–183.

16. A. I. Vogel, Elementary Practical Organic Chemistry: Qualitative Organic Analysis Part 2, second edition. Pearson, 1966, 96–106.

17. P. Ghosh, M. Das and S. Dhara, 2013, Indian Patent No. 566/KOL/2013.

18. S. P. Hoo, Q. L. Loh, Z. Yue, J. Fu, T.T. Y. Tan, C. Choong and P. P. Y. Chan, J Mat Chem B, 2013, 24, 3107–3117.

19. A. Aryaei, A. H. Jayatissa and A. C. Jayasuriya, J. Mech. Behav. Biomed. Mater., 2012, 5, 82–89.

20. (a) D.A. Puleo, R. Bizios, Biological Interactions on Materials Surfaces, Springer, 2009, chapter 1, page 7.(b) K. Wang, C. Zhou, Y. Hong and X. Zhang, Interface Focus, 2012, 2, 259–277; (c) C. F. Wertz and M. M. Santore, Langmuir, 2001, 17, 3006–3016.

21. (a) Y. Tamada and Y. Ikada, J. Colloid Interface Sci., 1993, 155, 334–339; (b) R. P Franke and S. Jung, Series on Biomechanics, 2012, 27, 51–58.

22. (a) L. Tirkkonen, H. Halonen, J. Hyttinen, H. Kuokkanen, H. Sievänen, A. M. Koivisto, B. Mannerström, G. K. Sándor, R. Suuronen, S. Miettinen and S. Haimi, J. R. Soc. Interface, 2011, 7, 1736–1747; (b) L. Francis, J. Venugopal, M.P. Prabhakaran, V. Thavasi, E. Marsano and S. Ramakrishna, Acta Biomater., 2010, 6, 4100–4109; (c) Y. Gotoh, K. Hiraiwa and M. Nagayama, Bone Miner., 1990, 8, 239–250.

23. C. A. Gregory, W. G. Gunn, A. Peister and D. J. Prockop, Anal Biochem., 2004, 329, 77–84.

24. (a) L. N. Wu, Y. Ishikawa, G. R. Sauer, B. R. Genge, F. Mwale, H. Mishima and R. E. Wuthier, J. Cell. Biochem., 1995, 57, 218–237; (b) H. C. Anderson, J. Cell Biol. 1969, 41, 59–72.

25. F. Pati, H. Kalita, B. Adhikari and S. Dhara, J. Biomed. Mater. Res. A, 2013, 101, 2526–2537.

26. (a) F. Di Palma, A. Guignandon, A. Chamson, M.H. Lafage-Proust, N. Laroche, S. Peyroche, L. Vico, A. Rattner, Biomaterials, 2005, 26, 4249–4257; (b) C. Wirth, B. Grosgogeat, C. Lagneau, N. Jaffrezic-Renault and L. Ponsonnet, Mater. Sci. Eng. C., 2008, 28, 990–1001.

27. J. I. Dawson and R. O. Oreffo, Arch. Biochem Biophys., 2008, 473, 124–131.

28. K. Lehle, S. Lohn, G. G. Reinerth, T. Schubert, J. G. Preuner, D. E.

Electronic Supplementary Information (ESI) available: See DOI: 10.1039/b000000x/

2.1 Preparation of chitosan fibers

Preliminary rheological characterization was performed to determine fiber forming ability of chitosan. Gelation kinetics of chitosan in alkaline condition (5% w/v NaOH) was assessed using Bohlin CVO Rheometer (Malvern Instrument, UK) with parallel plate geometry (20 mm diameter spindle) maintaining a gap of 500 µm. Briefly, complex viscosity (η∗) of chitosan upon addition of NaOH solution (from Merck, India), pH 13, was evaluated with time sweep measurement in an oscillatory mode at constant amplitude (0.01%) and frequency (1Hz) at 25°C. Blends of chitosan with DHF (Sigma Aldrich) at three different concentrations (3, 5 and 10 v/v%) were placed on rheometer plate and time sweep viscosity measurement was carried out to evaluate influence of DHF concentration on gel forming ability at 25 oC. Further, complex modulus measurement of chitosan–DHF blends were carried out as a function of temperature at constant frequency and shear stress of 1 Hz and 10 Pa, respectively, under linear visco-elastic region (LVR) upto 80 ^{o}C. Additionally, the gel strength was measured via amplitude sweep measurements (stress 0-100 Pa) at constant frequency of 2 Hz of the crosslinked chitosan formed by three different concentrations of DHF.

2.2.2 Crosslinking density, Swelling and Biodegradation study

Ninhydrin (2, 2-Dihydroxyindane-1, 3-dione) assay was performed to determine degree of crosslinking of chitosan fibers. In this assay, crosslinked and uncrosslinked chitosan fibers were boiled with ninhydrin (SRL Pvt. Ltd., India) solution and optical absorbance of the solution was recorded at 595 nm with a spectrophotometer (Recorders and Medicare Systems, India). Glycine (Merck, India) at various known concentrations was used as standard. Crosslinking density of the fibers was calculated as per the following equation.

% Crosslinking density = [(Cb-Ca)/Cb] x 100,

Where, Cb, Ca are the optical absorbance at 595 nm for chitosan fibers before and after crosslinking, respectively.

Swelling behavior of the chitosan fibers was measured in terms of change in weight as a function of immersion time. Dry scaffolds were weighed and soaked in phosphate-buffered solution, PBS (pH 7.4) at 37°C. They were taken out after 24 h and blotted dry with filter paper and again weighed. The percentage of swelling was calculated using the following formula-

% Swelling = [(wet weight – dry Weight)/ dry weight] × 100

Three replicates were performed and averaged.

In vitro degradation of crosslinked and uncrosslinked fibers was performed in PBS, pH 7.4 at 37 °C containing 1.5 µg/ml lysozyme (hen egg-white, Sigma-Aldrich) at specified time intervals (7, 14, 21 and 28 days).

3.1 Preparation of chitosan fibers

The complex viscosity of 6 wt % chitosan upon addition of 5% w/v NaOH solution increased instantaneously and reached a plateau in 400 s (S1a). Time sweep viscosity measurements of chitosan in presence of DHF with constant shear rate (10 s $^{-1}$) at 25 ^{o}C demonstrated absence of gelation which was also evident by insignificant change in viscosity (data not shown). In stark contrast, temperature sweep measurement revealed rapid increase in viscosity due to progressive liquid-gel transition at elevated temperature. Complex modulii of the blends increased significantly with increasing temperature and reached to maxima beyond 80 ^{o}C. Further, complex modulus was found to be strongly dependent on DHF concentration. However, complex modulii values were marginally higher for gels formed in 10% v/v DHF in comparison to 5% v/v during reaction progression. The increase in complex modulus with rise in temperature and concentration of crosslinker was mainly due to high degree of crosslinking of polymer by butenedial formed in situ through furan ring opening under acidic condition. Similar result was reported by Johnson et al. during gelation of alumina slurries using 1.5% chitosan solution and 10-100 mM DHF.[12] To assess gelation kinetics, elastic (G′) and viscous (G″) modulus of the chitosan blend using 5% v/v DHF was measured as shown in inset. The study clearly indicated that the G′ values increased significantly in comparison to G″ values mainly due to gel formation.

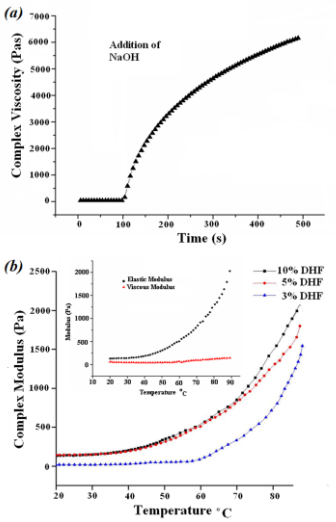

Fig. S1a Complex viscosity of 6 wt% chitosan after addition of 5% w/v NaOH at 25℃ as a function of time. Fig. S1b Complex modulus of chitosan-DHF blends under temperature sweep (0-80℃) at a constant frequency (1Hz) and shear stress (10Pa). b) Inset shows elastic and viscous modulus of 6 wt% chitosan with 5% v/v DHF blend as a function of temperature.

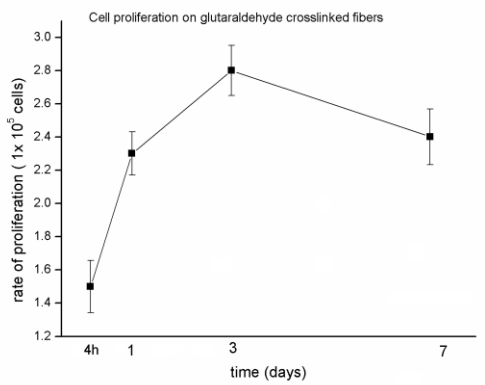

Fig. S2 MTT of hMSCs on chitosan fibers crosslinked with glutaraldehyde.

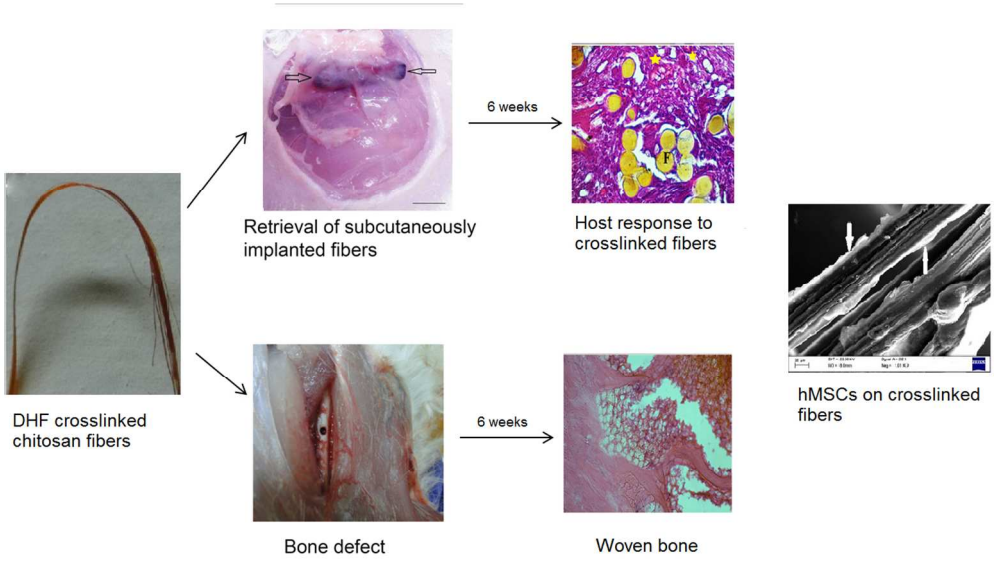

367x205mm (96 x 96 DPI)